Biosensors and Bioelectronics 144 (2019) 111640

Contents lists available at ScienceDirect

Biosensors and Bioelectronics

journal homepage: www.elsevier.com/locate/bios

Exploring electrochemistry of carbon nanodots and its application in noninvasive bacterial growth monitoring

Ritu Das[a], Neetu Singh[a,b,*]

[a] Centre for Biomedical Engineering, Indian Institute of Technology Delhi, Hauz Khas, New Delhi, 110016, India
[b] Department of Biomedical Engineering, All India Institute of Medical Sciences, Ansari Nagar, New Delhi, 110029, India

ARTICLE INFO

Keywords:
Carbon nanodots
Bacterial growth sensor
Electrochemical
Antibiotic susceptibility

ABSTRACT

Cost effective and miniaturized methods aiming for high throughput monitoring of bacterial growth are of great significance, especially for tracking disease progression in early stage as well as in screening antibiotic resistant species. Here, we demonstrate an electrochemical platform for noninvasive monitoring of bacterial growth by encapsulating bacterial cells and carbon nanodots in alginate microspheres. The synthesized carbon nanodots have been explored for electrochemical properties, and its redox properties have been utilized for developing bacterial growth monitoring platform. These synthesized CDs are sensitive to pH change and respond as change in redox potential over time as pH of the medium changes due to growth and metabolic activities of bacteria. We determined the bacterial growth kinetics by measuring the redox potential changes of the carbon nanodots over time. The developed platform has been demonstrated to detect the presence of bacteria, the difference in growth rates of bacteria and its susceptibility to the antibiotic with low bacterial counts (10^3 CFU) in 20 min; thus, redox properties of CDs has the potential to provide a sensitive detection platform.

1. Introduction

Carbon nanodots (CDs) have recently received considerable scientific attention as new member of carbon nanomaterial family. CDs are quasi-spherical nanoparticles with diameters in nanometers, possesses many advantages such as excellent photoluminiscence, small size, good conductivity, high solubility, chemical inertness, low toxicity, and resistant to photobleaching (Sun et al., 2006; Zheng et al., 2015; Zhu et al., 2013). Along with these properties, the economical and straightforward one-step synthesis of CDs makes them an attractive material for applications in biological imaging (Goh et al., 2012), sensing (Chandra and Singh, 2018, 2017; Kong et al., 2012), photocatalysis (Yu et al., 2016), drug delivery (Ding et al., 2015; Q. Wang et al., 2013), and photovoltaic devices (H. Lim et al., 2018; Xie et al., 2014).

CDs owe their wide array of applications to strong fluorescence that they exhibit and extensive studies are going on to explore the mechanism behind their photoluminescence (PL) (S. Zhu et al., 2015). Several studies have explored different aspects including the graphitic core, presence of functional groups, and type of carbon backbone to determine the phenomenon of PL of CDs. While, the photoluminescence properties of CDs are extensively studied, very few examples exist where the electrochemical properties of CDs are exploited for various applications. One such study includes tuning of electrochemical properties of CDs using various quinone for preparing and characterizing redox library of CDs. The synthesis of CDs was done by microwave assisted bottom up approach (Rigodanza et al., 2018). Similarly ascorbic acid and uric acid were utilized to obtain carbon dots for comparing the electrochemical properties of graphene and carbon quantum dot (C. S. Lim et al., 2015). From these studies it was evident that CDs possessed similar electrochemical properties as graphene. The detection of uranium using photophysical and electrochemical properties of graphene quantum dots with a detection limit of 0.56 μg/L and 2.0 μg/L respectively has also been reported (Guin et al., 2018). Most of the studies on CDs have utilized either quinone or graphene as precursor for synthesis of carbon dots. We utilized precursors of carbon and nitrogen form organic sources to synthesize CDs, which can have amine, carboxyl and hydroxyl groups on the surface making the surface sensitive to pH changes. These electrochemical properties of the synthesized CDs were studied to explore their application in developing electrochemical sensor for bacterial growth monitoring.

Electrochemical biosensor have emerged as the most prevalent form of sensing as they are economical and can be easily miniaturized, thus, enabling development of portable devices (C. Zhu et al., 2014). They require simpler equipment that can be easily integrated and provide user-friendly readout, require low sample volumes and usually have short sensing/readout time as they are based on electrochemical

* Corresponding author. Centre for Biomedical Engineering, Indian Institute of Technology Delhi, Hauz Khas, New Delhi-110016, India.
E-mail address: sneetu@iitd.ac.in (N. Singh).

https://doi.org/10.1016/j.bios.2019.111640
Received 30 May 2019; Received in revised form 11 August 2019; Accepted 26 August 2019
Available online 29 August 2019
0956-5663/

changes. Additionally, these can be easily multiplexed. Thus, electrochemical sensors are the most preferred type of sensors when easy, rapid and sensitive detection is required (Labib et al., 2016; Lavania et al., 2018; L. Wang et al., 2019). An important role of these sensors is towards rapid and sensitive detection of bacteria, these sensors can also be utilized for detection of bio-warfare agent (Das et al., 2015), environment and food contaminants (Das et al., 2019a, 2014) and clinically important pathogens (Das et al., 2019b; Lavania et al., 2018).

Rapid bacterial growth monitoring is important not only for clinical diagnosis, food and beverages industries, environmental monitoring but is also essential to curb misuse of antibiotics and help reduce antimicrobial susceptibility. Several approaches for characterizing bacterial growth such as cell counting on agar plates, microscopy and PCR produce accurate data but are often labor-intensive, time consuming and risks infecting the surrounding environment (Nemati et al., 2016; Zweitzig et al., 2013). Other optics-based techniques including measuring turbidity suffer from light scattering at too high concentration of cells leading to saturation of the signal. Some label free, rapid methods such as light-addressable potentiometric sensors, ionsensitive field-effect transistors shows high sensitivity but lacks miniaturization and rapid detection due to need of light source and positioning stage. Electrochemical approaches for bacterial growth monitoring includes, interdigital microelectrode biosensor for *in vitro* monitoring of two *Staphylococcus aureus* and two *Staphylococcus epidermidis* strains using impedance spectroscopy in 96-well microtiter plates (Paredes et al., 2013), and a biosensor for monitoring the biofilm formation of *Salmonella* and *Escherichia coli* (Liu et al., 2018). In the later work a glass substrate with interdigital microelectrodes and PDMS layer with micro cavities was used to record changes in electrochemical properties *via* impedance spectroscopy. The result clearly demonstrated that electrochemical changes can be used for detection of biofilm of *Salmonella* and *E. coli.* In yet another example, aptamer based sensor for growth and antibiotic susceptibility test for *E.coli* and *S. aureus* has been studied. Here, it was observed that overtime as the bacteria grows the capacitance increased yielding a growth curve. Using this technique growth curve with 10 CFU/mL bacteria was obtained and the platform was also utilized for identifying bacterial growth within 1 h (Jo et al., 2018). Currently available methods for Antimicrobial susceptibility testing (AST) includes broth dilution test, disk diffusion test, antimicrobial gradient test (includes commercially available E-test), automated instrument systems, mechanism specific systems, etc, with most of these requiring an average time of ~12 h for the test. VITEK utilizes pH change and other biochemical assay to determine AST, which involves complex procedure with low identification (Ligozzi et al., 2002). Another commonly used method, BACTEC, has been utilized for rapid testing and uses ^{14}C labeled nutrient for bacterial growth, requires closed environment, and is usually done in 24 h (Nonhoff et al., 2005). A comparision table of all the available methods is given in Table S1. Despite the availability of mentioned methods, there is still an unmet need to develop a rapid detection platform where low bacterial counts can be detected in a very short span of time.

Herein, we have developed a bacterial growth determination platform (Scheme 1), which can be used to perform antimicrobial susceptibility assay in short duration with low bacterial counts. The platform utilizes the redox properties of CDs, providing a sensitive bacterial growth monitoring platform. Here, CDs act as nanoprobe, which responds to pH changes in the media due to the growing bacteria. The electrochemical property of the synthesized carbon nanodots and the effect of pH on its redox behavior is thoroughly studied and then utilized to develop a non-invasive bacterial growth-monitoring sensor. The CDs are co-encapsulated with bacterial cells in alginate microspheres, which provides a 3D environment for better growth of the bacteria. The bacteria growing inside can then be easily detected by observing the changes in electrochemical properties of CDs. We hypothesized that sensing in a microsphere with an electrochemical nanoprobe in the close proximity of the growing bacterial cell will allow us to monitor small changes in the microenvironment. Such platforms can be more sensitive leading to detection of low number of bacteria compared to other methods generally used due to the simple reduction in volume of the growth environment.

2. Materials and methods

2.1. Carbon nanodots synthesis and encapsulation

Lyophilized *Agaricus bisporus* powder (0.6 g) and ethylenediamine (1 M) was mixed and sonicated in 10 mL deionized water, this solution was transferred to Teflon lined stainless steel vessel and heated in oven at 180 °C for 12 h. After 12 h, the vessel was cooled down, and the obtained resultant dark brown solution was centrifuged at 8000 rpm for 30 min. The supernatant collected was further purified to remove unreacted residues by dialysis using 3.5 kDa membrane in deionized water for 2 days. Finally, the purified carbon nanodot solution was stored at 4 °C in a refrigerator for further use.

The synthesized CDs were characterised using Transmission Electron Microscopy (TEM) to determine the size, X-ray Diffraction (XRD) and FTIR was performed to determine the atomic structure and functional groups on CDs. Zetapotenial was measured to determine the surface charge of the nanodots. To determine the electrochemical behavior cyclic voltamogramm (CV) was performed in 10 mM Tris buffer solution and in 5 mM potassium ferrocyanide and ferricyanide solution.

Carbon nanodot encapsulated microspheres were synthesized by mixing 0.5 mg/mL CDs with 1.0% sodium alginate and 0.9% NaCl in deionized water, this solution was dropped into 1.1% calcium chloride solution at a defined flow rate using syringe pump. The potential was generated at both ends by applying voltage of ~7000 V by power module. The drops of sodium alginate solution gets attracted towards the calcium chloride solution in petri plate having charge of opposite polarity, this results in generating dropplets, which are crosslinked as soon as they come in contact with $CaCl_2$ solution. The drops were further incubated for 20 min for proper completion of crosslinking and resulting in formation of microspheres.

2.2. Electrochemical studies of carbon nanodots

Electrochemical experiments were performed at room temperature using screen printed electrode having three electrode configuration. To determine the electrochemical properties of CDs, the cyclic voltamogramm (CV) of CDs was performed in 10 mM Tris buffer solution in the potential range of −1.0 V–1.0 V, at scan rate of 10 mV/s 0.5 mg/mL CDs solution was dropped on electrode surface covering the three electrode system to study the electrochemical properties of CDs. CV of CDs was also carried out in 0.1 M HCl containing 0.4 M KCl to confirm the formation of quinone structure in the synthesized carbon nanodots.

To study the effect of pH on redox properties of CDs, the pH of the CDs was artificially altered and CV was recorded. Then to study the affect of encapsulation and to ensure the encapsulation of CDs in alginate microspheres, bare CDs, alginate microspheres (Alg MS) with and without CDs (Alg MS/CDs) are electrochemically characterised using CV in 5 mM potasium ferrocyanide and ferricynaide solution. To study the stability, and electron transfer resistance CV at different scan rates were performed in 5 mM potasium ferrocyanide and ferricynaide solution. These microspheres are futher scanned using CV to study the effect of encapsulation on redox behavior of CDs in Tris buffer solution.

2.3. Electrochemical determination of bacterial growth

All bacterial cultures, *Pseudomonas aeruginosa (PA), Escherichia coli (E. coli), Salmonella typhi (ST),* and *Staphylococcus aureus (SA)* were first inoculated in Luria-Bertani (LB) broth and incubated at 37 °C/250 rpm for overnight. One percent inoculum of overnight grown culture was then sub-cultured in fresh LB broth. Following its absorbance at 600 nm

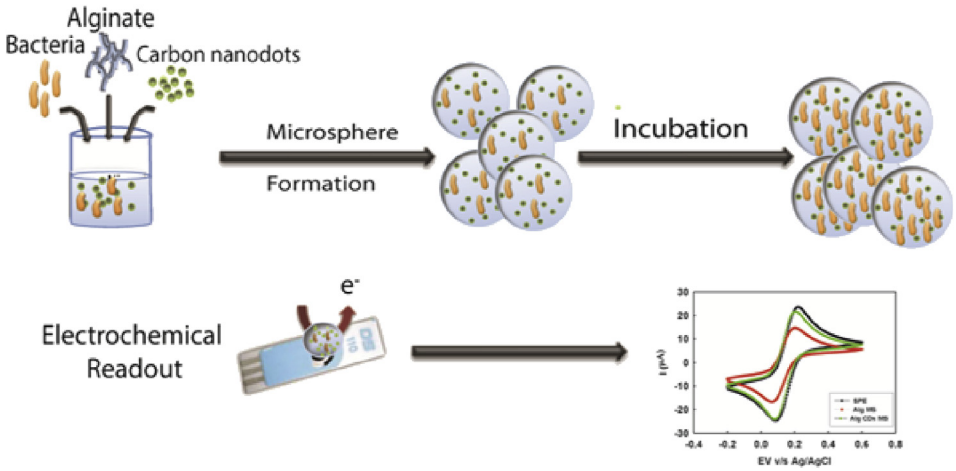

Scheme 1. Study design of development of CDs encapsulated microspheres for determination of microbial growth.

was constantly monitored for bacterial growth. Further the cell was harvested at O.D. ~1.0 and centrifuged at 7000 RPM for 7 min followed by two washes with distilled water and finally cells were diluted to get desired CFUs (8×10^8).

To monitor the growth of bacteria, bacterial cell with different cell numbers were co-encapsulated with CDs in alginate microspheres and allowed to incubate at 37 °C. To determine the bacterial growth CV was recorded at different time intervals to monitor the change in signal due to increase in cell number.

2.4. Antimicrobial susceptibility assay

To determine the drug resistant profile of the bacteria. *E. coli* and ampicillin resistant *E. coli* DH5α-pET strains (10^6 CFU/mL) were co-encapsulated with CDs in alignate microspheres with ampicillin (100 μg mL^{-1}) and incubated at 37 °C. Growth of both strains were monitored using CV over time.

3. Results and discussion

3.1. Characterization

The carbon nanodots were synthesized using an organic source. Briefly, 0.6 gm lyophilized powder of *Agaricus bisporus* was mixed with 1 M ethylenediamine and total volume was made up to 10 mL using deionized water. This solution was sonicated for 30 min and transferred to Teflon lined stainless steel autoclave vessel and heated at 180 °C for 12 h. After 12 h, the reaction was allowed to cool down at room temperature and resultant dark brown solution was collected and centrifuged at 12000 rpm for 30 min. The supernatent was collected and dialyzed in deinoized water for 48 h using 3.5 kDa cut-off dialysis tubing. After obtaining the pure carbon nanodots, they were thoroughly characterised for their size, charge, crystallinity and surface functional groups. In transmission electron microscopy (TEM), the size of synthesized CDs were found to be ~17 nm and were observed to be spherical and highly monodispersed (Fig. 1A). The charge present on particles was confirmed by zeta potential to be −9.85 mV (Figure S1A). X-ray Diffraction (XRD) (Fig. 1B) confirmed the amorphous nature of carbon nanodots. A prominent hump centered around ~2θ = 23° has been observed in the profile corresponding a set of sp^2 carbons-graphitic carbons with stacking faults indicating topological disorder in CDs. Presence of this single peak in the spectrum confirms the amorphous nature of the carbon nanodots. Fourier transform Infra-red (FTIR) spectroscopy was performed to determine the functional group present on the CD surface (Figure S1B). A broad peak was obtained, spanning from 3691 to 3002 cm^{-1} indicated stretching vibration of O–H and N–H. Peaks located at 1384 and 2919 cm^{-1} represent bending and stretching of C–H respectively. Presence of primary amine can be indicated by peak at 3406 cm^{-1} for N–H stretch, 1644 cm^{-1} for N–H bend and 1076 cm^{-1} for C–N stretch. Peak at 1153 cm^{-1} represents the stretching vibrations of C–O. Thus, the FTIR spectrum shows presence of amine, hydroxyl and carboxyl group commonly observed in carbon nanodots. Presence of carboxyls and amines renders pH sensitivity to the carbon nanodots as the functional groups may get protonated or deprotonated at varying pH. We confirmed the changes in the surface functional groups by monitoring the zeta potential of CDs at different pH. As can be observed from Figure S1C, the zeta potential changes from −2.58 to −9.85 mV on varying the pH from 4 to 7.5.

3.2. Encapsulation of CDs in alginate microscpheres

Since, we have synthesized the CDs as nanoprobe for developing a bacterial growth detection platform, we first encapsulated the CDs in a microsphere, which supports bacterial growth by providing an optimal microenvironment. For this 1% alginate solution along with 0.9% NaCl was mixed and filtered with 0.2 μm filter. 0.5 mg/mL of carbon nanodots and *E. coli* were mixed to the solution followed by crosslinking the solution with 1.1% $CaCl_2$ by maintaining the voltage of opposite potential. The microspheres were kept for 20 min in $CaCl_2$ solution and finally microspheres containing *E. coli* and CDs were collected and incubated in media containing Dulbecco's modified Eagle medium (DMEM) and Luria-Bertani medium (LB) at 37 °C in 96 well, flat bottom plate. The carbon nanodots did not aggregate and were well dispersed as indicated by their UV–Vis spectra, which was unaltered after the encapsulation (Figure S2).

3.3. Eletrochemical studies of carbon nanodots

After thoroughly characterizing the carbon nanodots and encapsulating them into an alginate microsphere, we investigated the conductive behavior by recording the CV of carbon nanodots encapsulated in alginate microspheres. First, the CV was recorded for carbon nanodots loaded alginate microspheres in 5 mM $K_4[Fe(CN)_6]^{-3/4}$ with 0.1 M KCl at scan rate of 10 mVs^{-1} on disposable carbon based screen printed electrode (SPE). Fig. 1C shows the CV of blank SPE, alginate microspheres (Alg MS), CD-loaded alginate microspheres (Alg CDs MS) and bare CDs. An increase in current can be observed on encapsulating CDs in Alg MS when compared with CV of SPE and Alg MS. The encapsulation of CDs reduces the current as seen from the CVs of bare CDs and Alg CDs MS. However, the current signal even after encapsulation was still significantly high in case of Alg CDs MS when compared with Alg MS, clearly indicating that Alg CDs MS can be

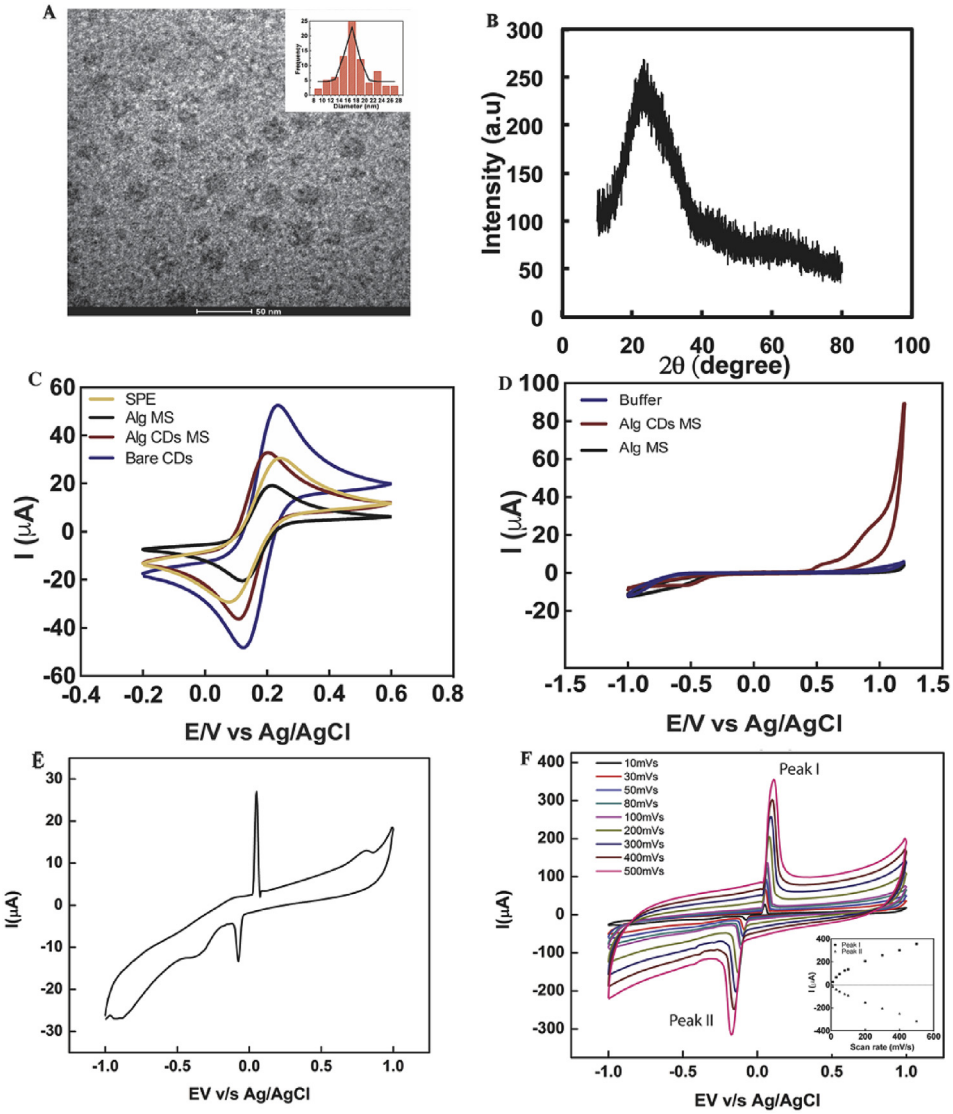

Fig. 1. (A) Transmission electron microscopy image, (B) XRD pattern of carbon dots, (C) Cyclic voltammogram of SPE, Alg MS, Alg CDs MS and bare CDs in 5 mM $K_4[Fe(CN)_6]^{-3/4}$, (D) Cyclic voltammogram of buffer, SPE, Alg MS and Alg/CDs MS in 10 mM Tris buffer solution, (E) CV of CDs in 0.1 M HCl with 0.4 M KCl and (F) CV at different scan rate in 0.1 M HCl with 0.4 M KCl (Inset: linear relation of increase in current at different scan rate).

utilized for monitoring any electrochemical changes. The stability and electron transfer behavior was studied at different scan rate in 5 mM $K_4[Fe(CN)_6]^{-3/4}$ with 0.1 M KCl (10, 20, 50, 100, 150, 200, 300, 400, and 500 mV/s) on disposable carbon based screen printed electrode (SPE) **(**Figure S3**).** The reaction was found to have fast electron transfer indicating the stability of CDs as the peak pattern of CV curves remains same. The peak current increases linearly as a function of square root of scan rates representing the easy electron transfer from microspheres to electrode surface and vice versa. A faster scan rate leads to decrease in diffusion layer and an increase in peak current with slight shift in the peak current shows the reaction is diffusion-limited and electron transfer process is quasi reversible. Further, the electrochemical properties were also explored by recording CV in 10 mM Tris buffer solution. Redox peaks were observed at 0.54 and −0.53 V indicating redox active nature of CDs (Fig. 1D). The redox activity can be predicted due to quinone structure and peripheral functional moieties present on CDs. Fig. 1E represents the CV of CDs when carried out in 0.1 M HCl containing 0.4 M KCl, it confirms the formation of quinone structure, as two sharp peaks can be seen at 0.045 V and −0.07 V depicting characteristics peaks of quinones (Fig. 1F). This behavior is actually due to charge transfer of peripheral functional moieties that were analogous to quinone derivatives having properties of aromatic compounds (Ishioka et al., 2001; Newman and Lilje, 1979; Tian et al., 2009) and carboxylic acid moieties on the CDs surfaces. Certainly, for clear understanding of the molecular mechanism, further studies are needed to unravel the detailed structure of CDs.

3.4. Effect of pH on electrochemical properties of carbon nanodots

Before determining the changes in CDs electrochemical properties by bacterial growth, we evaluated the effect of pH on the redox properties of CDs by recording the CV of CDs encapsulated in microspheres at different pH. As the redox properties depend upon the functional groups, pH of the solution is expected to have a strong influence on the electrochemical properties of carbon nanodots. During CV, with the decrease in pH of buffer solution, a gradual increase in the reduction potential has been observed, indicating that the acidic conditions were beneficial to the reduction process (Figure S4). This gradual increase in the reduction potential suggests the involvement of two proton and two electron redox reaction at electrode surface leading to potential shift. A plot of solution potential *vs.* pH (from pH 7.5 to 4) showed a linear relationship with the slope of 11.52 mV per pH unit, suggesting the

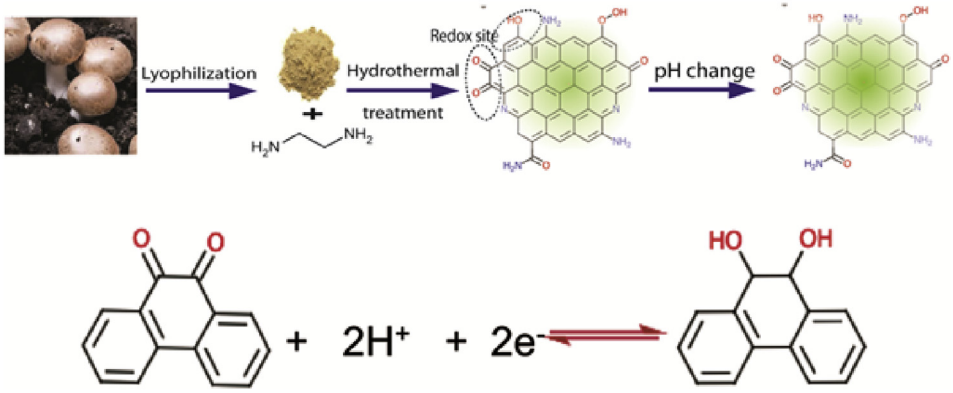

Scheme 2. The preparation of CDs from *Agaricus bisporus*; (b) the electron transfer of quinone redox sites.

participation of protons (Scheme 2) (Ishioka et al., 2001; Tian et al., 2009). We hypothesized that this sensitivity of the electrochemical behavior of CDs to the solution pH can be exploited to monitor bacterial growth as it is well established that bacterial growth and metabolic activities results in lowering of pH of the growth media.

3.5. Monitoring bacterial growth

First, the bacterial viability in alginate microsphere was confirmed by staining the cells using acridine orange dye, which stains only live bacteria. The microspheres were incubated at 37 °C and were monitored at different time intervals using fluorescence microscopy. The bacterial growth at 0 h, 6 h, and 12 h were compared and formation of colonies inside microspheres after 6 h was observed under bright field and fluorescent microscope (Figure S5 and S6).

After confirming the habitable environment of microspheres, pH change of the microenvironment due to growth of *E. coli* was evaluated. Performing CV of alginate microsphere and CDs loaded alginate microsphere confirmed the encapsulation of carbon nanodots inside the microspheres. For determining the change in pH due to growing bacteria *via* electrochemical readouts, microspheres encapsulated with CDs and *E. coli* (10^6 CFU/mL) were incubated in 96 well plate at 37 °C and CV of microspheres was recorded at different time intervals (0, 1, 2, 4, 6 h). And with increase in incubation time a gradual increase in the reduction potential was observed due to the change in pH of the microenvironment resulting from growth of bacteria. The shift in reduction peak with increase in incubation time represents a decrease in pH, similar to the changes observed in Fig. 2A. Therefore, this establishes a correlation between change in pH due to bacterial growth and the observed reduction potential **(**Fig. 2B**)**. To observe the interference of dead cells in the signal, acridine orange staining was performed and a significant number (~90%) of live cells were observed even after 6 h **(**Figure S7**)**. Interestingly, there was loss in current signal after 6 h but it was still significant to monitor growth. To confirm the real time pH change in the microspheres the study was validated by previously reported method by our group and present results correlated with the previous study (Chandra and Singh, 2018). The global pH of the solution was changed (from pH 7 to pH 5.5) and measured with pH meter to obtain the pH values of the sample. The pH measured by the pH meter was then plotted against fluorescence intensity ratio (green/blue) and reduction potential (Figure S9A). It was observed that as the bacterial cell growth increases the fluorescence intensity ratio (green/blue) increases and a gradual increase in reduction potential is observed. In addition the pH of growing bacteria solution was measured to establish that bacterial growth (increasing absorbance) indeed results in lowering of pH over time (Figure S9B). These results confirmed the real time change in pH value of the microenvironment. It is important to note that the change in pH is rather slow and not easy to monitor globally by a pH meter and hence an in situ sensor like the GQDs provide an unprecedented method to monitor it in real time as it can measure the local pH even when the global pH remains unaltered (unmeasurable). To establish the lowest duration of time required for detecting the changes we monitored in the change in potential over time. As indicated by **Fig. 3A** we observed changes in as less as 20 min. Following this, we investigated the lowest number of bacteria that can be detected in 20 min by the alginate-CD microspheres and were delighted to observe that a low concentration of bacteria (10^3 CFU) also resulted in a significant change in pH. This change was easily detected by the percentage change in potential (Fig. 3B), thus, clearly suggesting that the developed platform has the ability to rapidly detect low bacterial concentrations. It is important to note that this rapid readout for low concentration of bacteria is unprecedented. To compare the present method with the standard method of bacterial growth monitoring, calibration curve for bacterial growth by change in reduction potential was compared with change in absorbance over time **(**Figure S8**)**. A linear change in absorbance as well as in reduction potential was evident. Moreover, the potential change with respect to time was significantly higher as compared to absorbance change with respect to time. Together these results signify that present method can be used as a potential tool for monitoring the growth rate.

3.6. Comparison of bacterial growth rate

After successfully monitoring the growth of bacteria, we investigated if the platform can be utilized to differentiate bacteria based on the growth rate. Growth rates of *Pseudomonas aeruginosa, Escherichia coli, Salmonella typhi,* and *Staphylococcus aureus* were electrochemically monitored. CV of *P. aeruginosa,* co-encapsulated with CDs showed a very less shift in reduction potential after 1 h incubation of culture when compared with *E. coli, S. typhi and S. aureus* (Figure S10A, S10B, S10C **and** Fig. 4A).

3.7. Performance of antibiotic susceptibility assay

We further evaluated the applicability of the platform in differentiating an antibiotic resistant and non-resistant strains. CV of *E. coli* (non-resistant) and *E. coli* + pET32 (resistant) encapsulated in microsphere with 4 μg mL^{-1} ampicillin was recorded at 0 h and 20 min. No peak shift was observed in case of *E. coli* when compared with *E. coli* + pET32 due to presence of ampicillin, suggesting that the resistant bacteria were growing while the non-resistant were in a lag phase (Fig. 4B). This clearly indicates the ability of the system to differentiate between antibiotic resistant and non-resistant bacteria in a short time of 20 min. The CV for longer time indicated the unaffected growth of resistant *E. coli* strain in the presence of antibiotic as even after 4 h the non-resistant strain did not show increase in potential and the resistant strain had significant increase in potential (Fig. 4C).

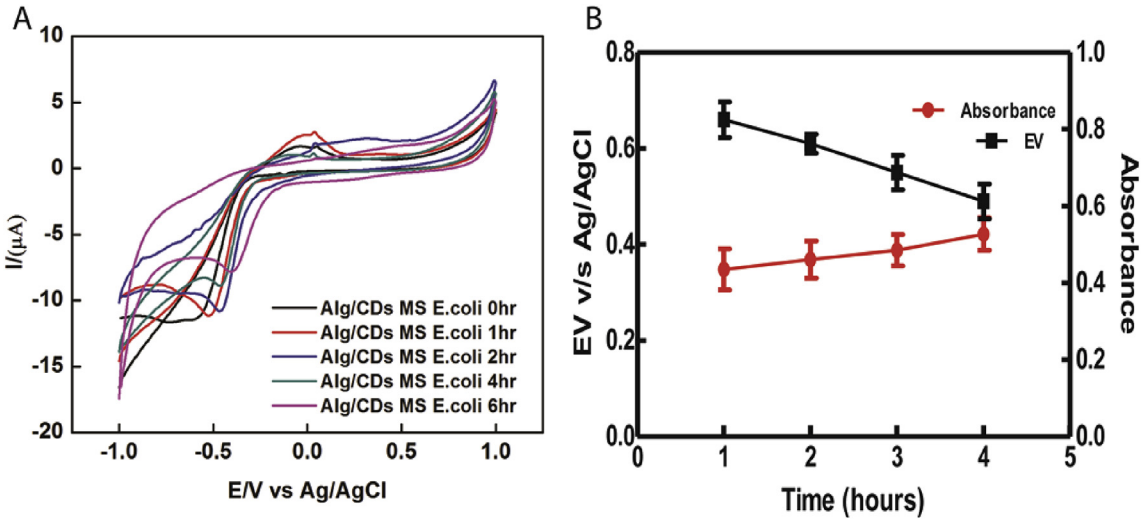

Fig. 2. (A) CV of Alg/CDs MS *E. coli* measured at different time intervals and (B) Plot showing change in potential and absorbance at different time intervals.

4. Conclusion

In the present study, the electrochemical properties of the CDs were explored to develop a reliable and highly sensitive platform for monitoring bacterial growth. The redox property of the synthesized CDs was found to be highly sensitive to pH change. This unique property of pH sensitive CDs helped in monitoring realtime pH change in the micromilieu due to bacteria growth thus enabling development of a rapid bacterial growth detection method. Using this platform, a low bacterial count of $< 10^3$ CFU/mL was detected in less than 20 min. The platform was able to differentiate slow and fast growing bacteria along with antibiotic resistant *vs.* non-resistant bacteria. Although only four bacterial strains are studied here we envision that the developed platform is universal and can be used for rapid high throughput analysis of multiple samples for antimicrobial susceptibility testing with multiple combinations of antibiotics, providing information about the best possible effective antibiotic combination.

Author contributions

RD performed the experiments and both authors have conceptualized, discussed and written the manuscript.

Funding sources

The work was funded by IITD grand challenge project MI01798.

CRediT authorship contribution statement

Ritu Das: Conceptualization, Methodology, Data curation, Formal analysis, Software, Writing - original draft, Writing - review & editing. **Neetu Singh:** Conceptualization, Methodology, Supervision, Formal analysis, Validation, Writing - review & editing, Project administration, Investigation, Funding acquisition, Resources, Visualization.

Declaration of competing interest

The authors declare that they have no known competing financial interests or personal relationships that could have appeared to influence the work reported in this paper.

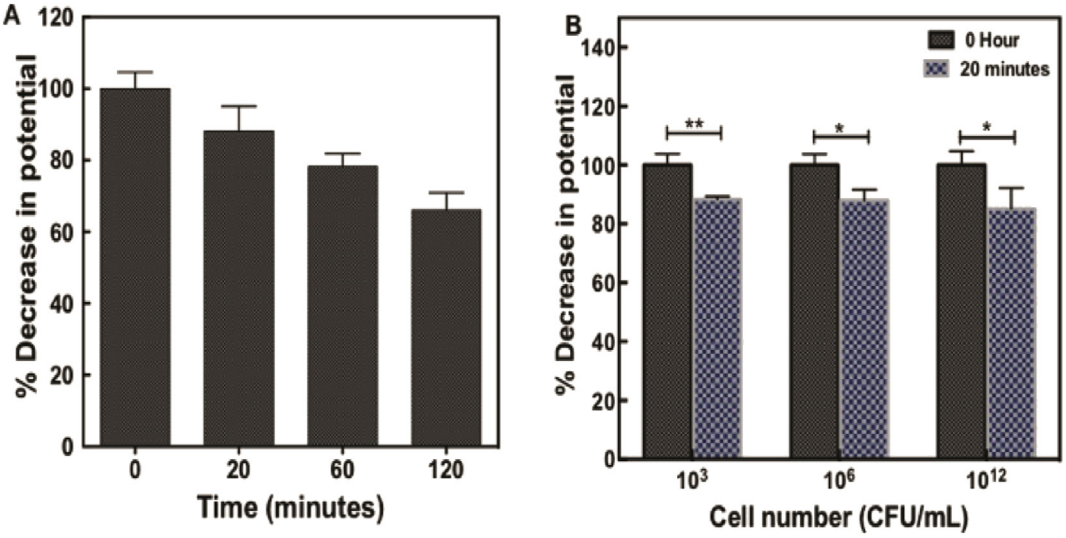

Fig. 3. (A) Plot showing percentage change in potential with respect to time on co-encapsulation 10^{12} CFU/mL with CDs in alginate microgels, (B) Plot showing percentage decrease in potential with 10^3, 10^6 and 10^{12} CFU/mL encapsulated with CDs in alginate microgels monitored at 0 and 20 min of incubation.

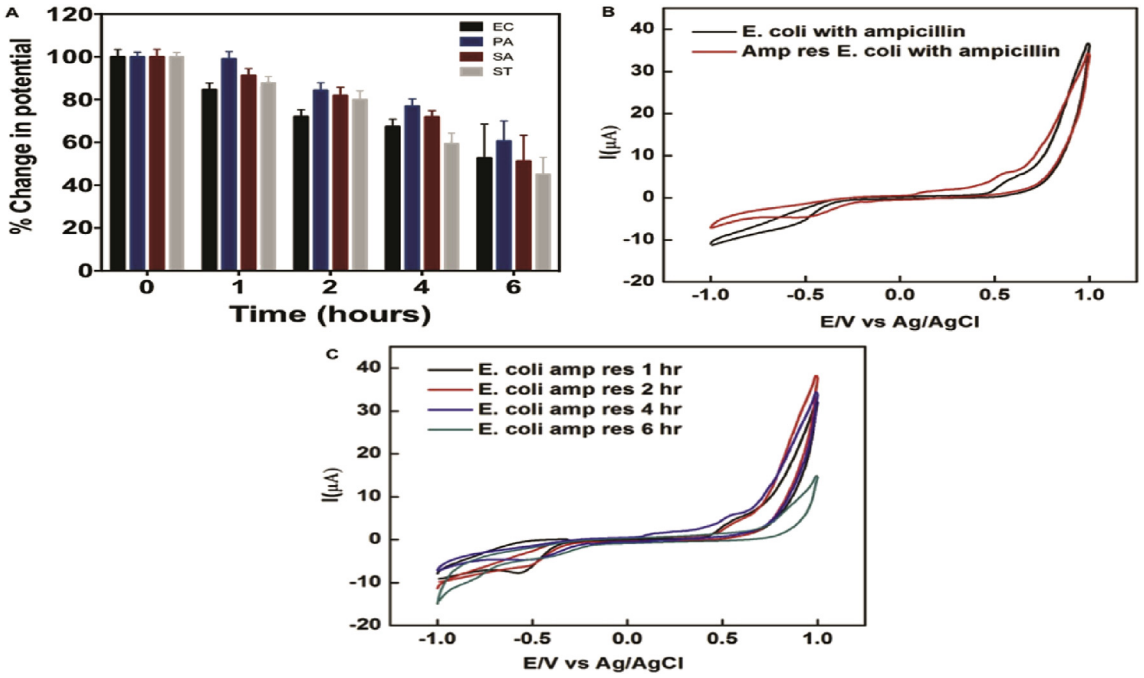

Fig. 4. (A) Plot representing comparison of growth rate of *E. coli, P. aeruginosa, S. aureus* and *S. typhi* based on decrease in potential with respect to time, (B) CV of *E. coli* and ampicillin resistant *E. coli* in presence of ampicillin (C) CV of Ampicillin resistant *E. coli* measured at different time points.

Acknowledgment

We acknowledge Central Research facility and Nanoscale Research Facility at IIT, Delhi. We acknowledge Mr Akshay Joshi and Ms Parul Sirohi for their help during synthesis and purification of CDs.

Appendix A. Supplementary data

Supplementary data to this article can be found online at https://doi.org/10.1016/j.bios.2019.111640.

References

Chandra, A., Singh, N., 2018. Bacterial growth sensing in microgels using pH-dependent fluorescence emission. Chem. Commun. 54, 1643–1646.
Chandra, A., Singh, N., 2017. Biocompatible fluorescent carbon dots for ratiometric intracellular pH sensing. ChemistrySelect 2, 5723–5728.
Das, R., Dhiman, A., Kapil, A., Bansal, V., Sharma, T.K., 2019a. Aptamer-mediated colorimetric and electrochemical detection of Pseudomonas aeruginosa utilizing peroxidase-mimic activity of gold. NanoZyme 1–10. https://doi.org/10.1007/s00216-018-1555-z.
Das, R., Dhiman, A., Mishra, S.K., Haldar, S., Sharma, N., Bansal, A., Ahmad, Y., Kumar, A., Tyagi, J.S., Sharma, T.K., 2019b. Structural switching electrochemical DNA aptasensor for the rapid diagnosis of tuberculous meningitis. IJN 14, 2103.
Das, R., Goel, A.K., Sharma, M.K., Bioelectronics, S.U.B.A., 2015. 2015. Electrochemical DNA sensor for anthrax toxin activator gene atxA-detection of PCR amplicons. Biosens. Bioelectron. 74, 939–946. https://doi.org/10.1016/j.bios.2015.07.066.
Das, R., Sharma, M.K., Rao, V.K., Bhattacharya, B.K., Garg, I., Venkatesh, V., Upadhyay, S., 2014. An electrochemical genosensor for Salmonella typhi on gold nanoparticles-mercaptosilane modified screen printed electrode. J. Biotechnol. 188, 9–16. https://doi.org/10.1016/j.jbiotec.2014.08.002.
Ding, H., Du, F., Liu, P., Chen, Z., Shen, J., 2015. DNA–carbon dots function as fluorescent vehicles for drug delivery. ACS Appl. Mater. Interfaces 7, 6889–6897.
Goh, E.J., Kim, K.S., Kim, Y.R., Jung, H.S., Beack, S., Kong, W.H., Scarcelli, G., Yun, S.H., Hahn, S.K., 2012. Bioimaging of hyaluronic acid derivatives using nanosized carbon dots. Biomacromolecules 13, 2554–2561.
Guin, S.K., Ambolikar, A.S., Guin, J.P., Neogy, S., 2018. Exploring the excellent photophysical and electrochemical properties of graphene quantum dots for complementary sensing of uranium. Sens. Actuators B Chem. 272, 559–573.
Ishioka, T., Uchida, T., Teramae, N., 2001. Analysis of the redox reaction of 9, 10-phenanthrenequinone on a gold electrode surface by cyclic voltammetry and time-resolved Fourier transform surface-enhanced Raman scattering spectroscopy. Anal. Chim. Acta 449, 253–260.
Jo, N., Kim, B., Lee, S.-M., Oh, J., Park, I.H., Jin Lim, K., Shin, J.-S., Yoo, K.-H., 2018. Aptamer-functionalized capacitance sensors for real-time monitoring of bacterial growth and antibiotic susceptibility. Biosens. Bioelectron. 102, 164–170.
Kong, B., Zhu, A., Ding, C., Zhao, X., Li, B., Tian, Y., 2012. Carbon dot-based inorganic–organic nanosystem for two-photon imaging and biosensing of pH variation in living cells and tissues. Adv. Mater. 24, 5844–5848.
Labib, M., Sargent, E.H., Kelley, S.O., 2016. Electrochemical methods for the analysis of clinically relevant biomolecules. Chem. Rev. 116, 9001–9090.
Lavania, S., Das, R., Dhiman, A., Myneedu, V.P., Verma, A., Singh, N., Sharma, T.K., Tyagi, J.S., 2018. Aptamer-based TB antigen tests for the rapid diagnosis of pulmonary tuberculosis: potential utility in screening for tuberculosis. ACS Infect. Dis. 4, 1718–1726.
Ligozzi, M., Bernini, C., Bonora, M.G., de Fatima, M., Zuliani, J., Fontana, R., 2002. Evaluation of the VITEK 2 system for identification and antimicrobial susceptibility testing of medically relevant gram-positive cocci. J. Clin. Microbiol. 40, 1681.
Lim, C.S., Hola, K., Ambrosi, A., Zboril, R., Pumera, M., 2015. Graphene and carbon quantum dots electrochemistry. Electrochem. Commun. 52, 75–79.
Lim, H., Liu, Y., Kim, H.Y., Son, D.I., 2018. Facile synthesis and characterization of carbon quantum dots and photovoltaic applications. Thin Solid Films 660, 672–677.
Liu, L., Xu, Y., Cui, F., Xia, Y., Chen, L., Mou, X., Lv, J., 2018. Monitoring of bacteria biofilms forming process by in-situ impedimetric biosensor chip. Biosens. Bioelectron. 112, 86–92.
Nemati, M., Hamidi, A., Dizaj, S.M., Javaherzadeh, V., Lotfipour, F., 2016. An overview on novel microbial determination methods in pharmaceutical and food quality control. Adv. Pharmaceut. Bull. 6, 301.
Newman, M.S., Lilje, K.C., 1979. Synthesis of 9-bromo derivatives of 4, 5-, 2, 7-, and 3, 6-dimethyl-and 2, 4, 5, 7-and 3, 4, 5, 6-tetramethylphenanthrenes. J. Org. Chem. 44, 4944–4946.
Nonhoff, C., Rottiers, S., Struelens, M.J., 2005. Evaluation of the Vitek 2 system for identification and antimicrobial susceptibility testing of Staphylococcus spp. Clin. Microbiol. Infect. 11, 150–153.
Paredes, J., Becerro, S., Arizti, F., Aguinaga, A., Del Pozo, J.L., Arana, S., 2013. Interdigitated microelectrode biosensor for bacterial biofilm growth monitoring by impedance spectroscopy technique in 96-well microtiter plates. Sens. Actuators B Chem. 178, 663–670. https://doi.org/10.1016/j.snb.2013.01.027.
Rigodanza, F., Đorđević, L., Arcudi, F., Prato, M., 2018. Customizing the electrochemical properties of carbon nanodots by using quinones in bottom-up synthesis. Angew. Chem. 130, 5156–5161.
Sun, Y.-P., Zhou, B., Lin, Y., Wang, W., Fernando, K.S., Pathak, P., Meziani, M.J., Harruff, B.A., Wang, X., Wang, H., 2006. Quantum-sized carbon dots for bright and colorful photoluminescence. J. Am. Chem. Soc. 128, 7756–7757.
Tian, L., Ghosh, D., Chen, W., Pradhan, S., Chang, X., Chen, S., 2009. Nanosized carbon particles from natural gas soot. Chem. Mater. 21, 2803–2809.
Wang, L., Yang, R., Li, J., Qu, L., Harrington, P. de B., 2019. A highly selective and sensitive electrochemical sensor for tryptophan based on the excellent surface adsorption and electrochemical properties of PSS functionalized graphene. Talanta 196, 309–316.
Wang, Q., Huang, X., Long, Y., Wang, X., Zhang, H., Zhu, R., Liang, L., Teng, P., Zheng, H., 2013. Hollow luminescent carbon dots for drug delivery. Carbon 59, 192–199.
Xie, C., Nie, B., Zeng, L., Liang, F.-X., Wang, M.-Z., Luo, L., Feng, M., Yu, Y., Wu, C.-Y., Wu, Y., 2014. Core–shell heterojunction of silicon nanowire arrays and carbon

quantum dots for photovoltaic devices and self-driven photodetectors. ACS Nano 8, 4015–4022.
Yu, H., Shi, R., Zhao, Y., Waterhouse, G.I., Wu, L.Z., Tung, C.H., Zhang, T., 2016. Smart utilization of carbon dots in semiconductor photocatalysis. Adv. Mater. 28, 9454–9477.
Zheng, X.T., Ananthanarayanan, A., Luo, K.Q., Chen, P., 2015. Glowing graphene quantum dots and carbon dots: properties, syntheses, and biological applications. Small 11, 1620–1636.
Zhu, C., Yang, G., Li, H., Du, D., Lin, Y., 2014. Electrochemical sensors and biosensors based on nanomaterials and nanostructures. Anal. Chem. 87, 230–249.
Zhu, S., Meng, Q., Wang, L., Zhang, J., Song, Y., Jin, H., Zhang, K., Sun, H., Wang, H., Yang, B., 2013. Highly photoluminescent carbon dots for multicolor patterning, sensors, and bioimaging. Angew. Chem. Int. Ed. 52, 3953–3957.
Zhu, S., Song, Y., Zhao, X., Shao, J., Zhang, J., Yang, B., 2015. The photoluminescence mechanism in carbon dots (graphene quantum dots, carbon nanodots, and polymer dots): current state and future perspective. Nano Res. 8, 355–381.
Zweitzig, D.R., Riccardello, N.M., Morrison, J., Rubino, J., Axelband, J., Jeanmonod, R., Sodowich, B.I., Kopnitsky, M.J., O'Hara, S.M., 2013. Measurement of microbial DNA polymerase activity enables detection and growth monitoring of microbes from clinical blood cultures. PLoS One 8, e78488.